Pattern Detection, Monte Carlo Simulation & ANN Applications in Vertical Two-phase CO_2 Flow

Hakki Karaman

08.07.2021

Goals & Outline

Main Goal: Improving the accuracy of void fraction ratio estimations of bubbly flow of vertical two-phase CO_2 flow by using the high speed camera images

Outline of the presentation:

- Improving 2D bubble detection of Shai's pipeline with geometric-based rotation invariant pattern detection algorithms
- Improving 3D reconstruction of bubbles with Monte Carlo simulations and ANN (artificial neural networks)
- Further Ideas for the future analyses of different flow regimes and experimental setup

Why Rotation Invariant Bubble Detection?

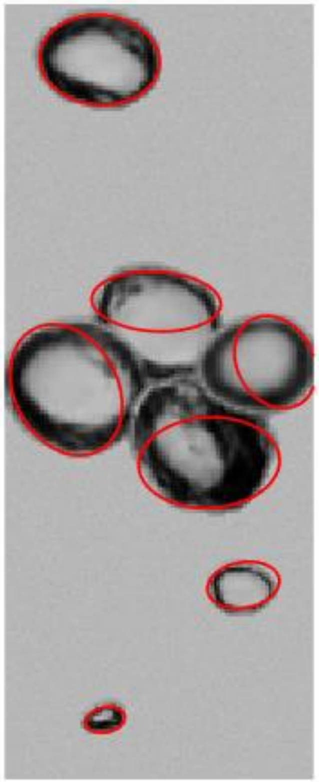

Standard ellipse fitting algorithm finds an ellipse that minimizes vertical mean square error (MSE)

Algebraic Error vs. Geometric Error

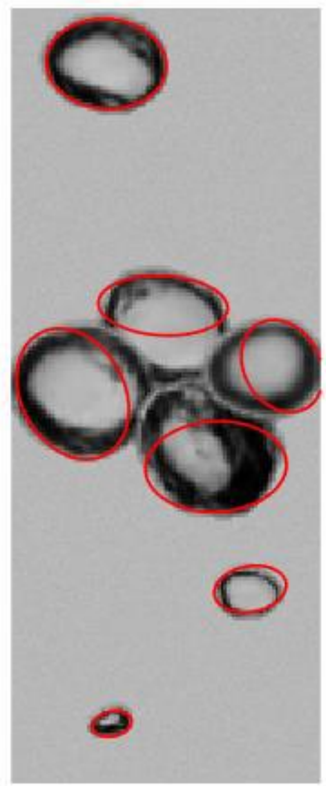

Fitting Algorithms finds the curve that minimizes MSE

i.e.

$$\min_{curve} \frac{1}{n}\sum_{i=1}^{n} {Error_i}^2$$

Defining algebraic error vs. geometric error

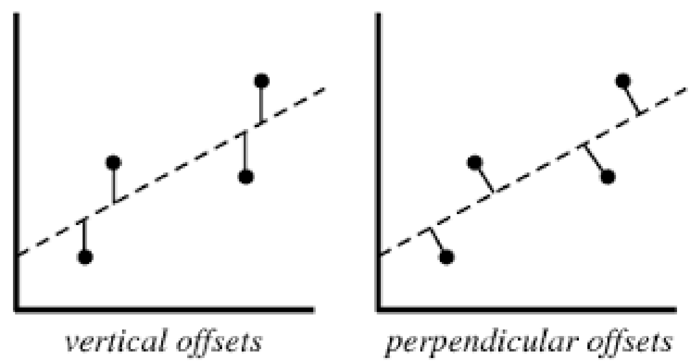

Standard ellipse fitting algorithm finds an ellipse that minimizes vertical MSE

Taubin's Method for Implicit Quadrics

2D Implicit Quadric Equation $\begin{bmatrix} c_0 & c_1 & c_2 & c_3 & c_4 & c_5 \end{bmatrix} \begin{bmatrix} 1 \\ x \\ y \\ x^2 \\ xy \\ y^2 \end{bmatrix} = \underline{\boldsymbol{c}}^{\boldsymbol{T}} \underline{\mathbf{X}} = \mathbf{f}(\mathbf{x}, \mathbf{y}) = 0$

Ellipse condition: $c_4{}^{\mathbf{2}} - 4 \cdot c_3 \cdot c_5 < 0$

$$\lambda = \boldsymbol{d}^{\mathbf{2}} \approx \frac{\boldsymbol{f}(\boldsymbol{x}, \boldsymbol{y})^{\mathbf{2}}}{\|\boldsymbol{\nabla f}(\boldsymbol{x}, \boldsymbol{y})\|^{\mathbf{2}}} = \frac{\underline{\boldsymbol{c}}^{\boldsymbol{T}} \underline{\underline{\boldsymbol{M}}}\, \underline{\boldsymbol{c}}}{\underline{\boldsymbol{c}}^{\boldsymbol{T}} \underline{\underline{\boldsymbol{N}}}\, \underline{\boldsymbol{c}}}$$

$\lambda :=$ Geometric MSE
d $:=$ Geometric RMSE

Taubin 1991 - Estimation of Planar Curves, Surfaces, and Nonplanar Space Curves Defined by Implicit Equations

Taubin's Method for Implicit Quadrics

$$\underline{\underline{\boldsymbol{M}}}_{6\times 6} := \frac{1}{n}\sum_{i=1}^{n} \underline{\mathbf{X}}_i \underline{\mathbf{X}}_i^{\boldsymbol{T}} = \frac{1}{n}\sum_{i=1}^{n} \begin{bmatrix} 1 \\ x_i \\ y_i \\ {x_i}^2 \\ x_i y_i \\ {y_i}^2 \end{bmatrix} \begin{bmatrix} 1 & x_i & y_i & {x_i}^2 & x_i y_i & {y_i}^2 \end{bmatrix}$$

$$\underline{\underline{\boldsymbol{N}}}_{6\times 6} := \frac{1}{n}\sum_{i=1}^{n} \underline{\underline{\boldsymbol{DX}}}_i \underline{\underline{\boldsymbol{DX}}}_i^{\boldsymbol{T}} = \frac{1}{n}\sum_{i=1}^{n} \begin{bmatrix} 0 & 0 \\ 1 & 0 \\ 0 & 1 \\ 2x_i & 0 \\ y_i & x_i \\ 0 & 2y_i \end{bmatrix} \begin{bmatrix} 0 & 1 & 0 & 2x_i & y_i & 0 \\ 0 & 0 & 1 & 0 & x_i & 2y_i \end{bmatrix}$$

Generalized Eigenvalue Problem

$$\underline{\underline{\boldsymbol{M}}}\,\underline{\boldsymbol{c}} = \lambda\,\underline{\underline{\boldsymbol{N}}}\,\underline{\boldsymbol{c}}$$

There are 6 eigenvalue λ:

- λ_{min} is the Geometric MSE
- Corresponding eigenvector $\underline{\boldsymbol{c}}$ to λ_{min} are the coefficients of the optimal ellipse

Results with Synthetic Data

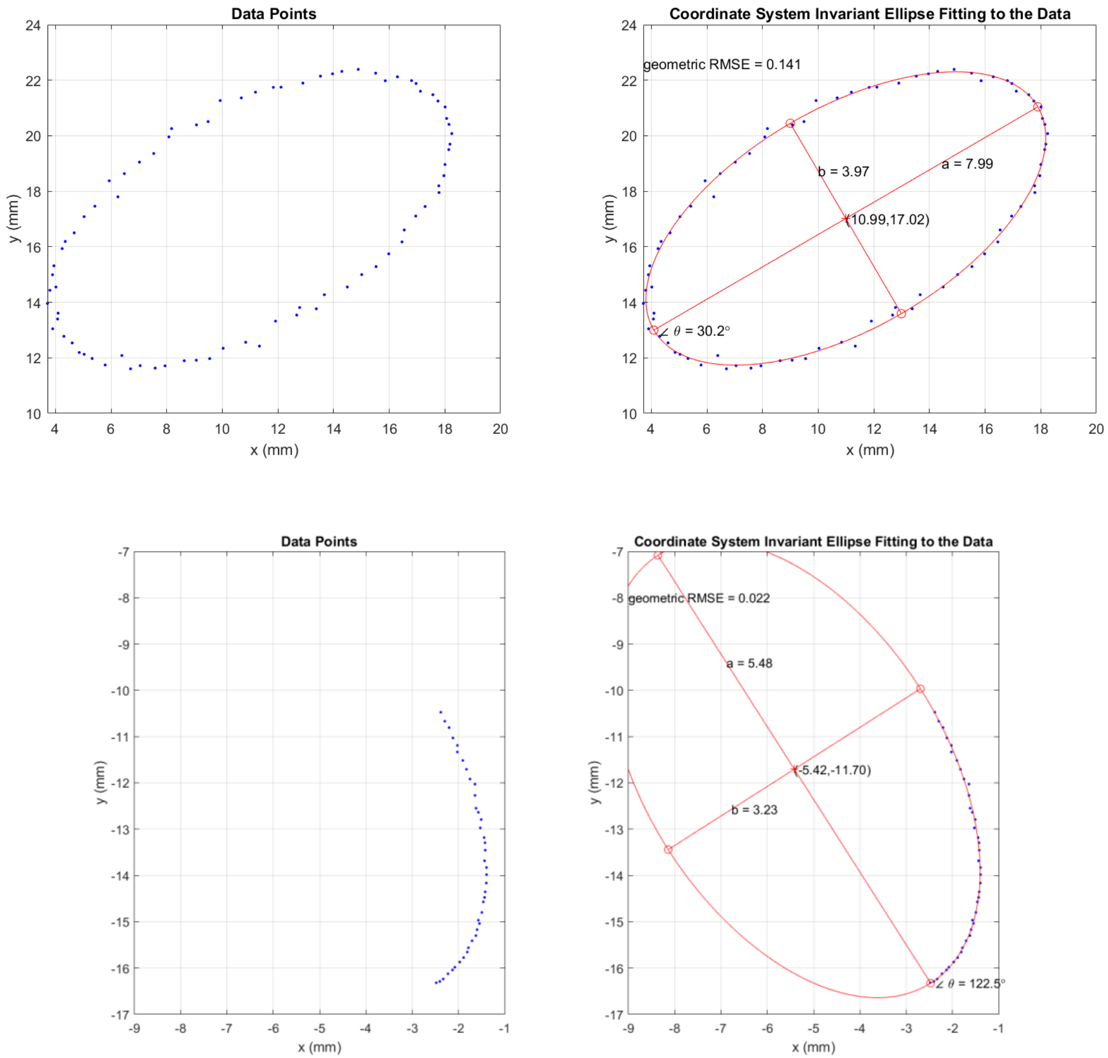

Results of Fitting Rotation Invariant Ellipse to the synthetic Data

Rotation Invariant Bubble Detection Results

Before After

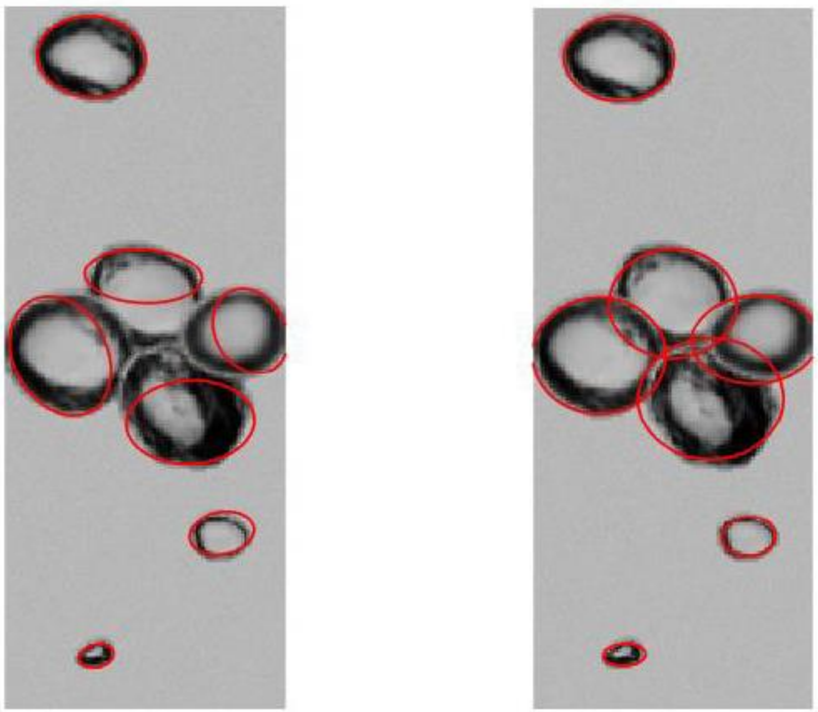

(a) (b)

Bubble detection pipeline result (a) with regionprops (standard ellipse fitting of MATLAB) and (b) with geometric ellipse fitting implementation

- traditional ellipse fitting algorithm minimizes the total vertical error
- my implementation minimizes the orthogonal/ geometric error

From 2D Images to 3D Bubbles

$$\text{Void } fraction\,ratio = \frac{1}{\#frames} \sum_{i=1}^{\#frames} \frac{Total\ volume\ of\ the\ bubbles\ in\ frame\_i}{Volume\ of\ the\ inner\ tube\ in\ frame\_i}$$

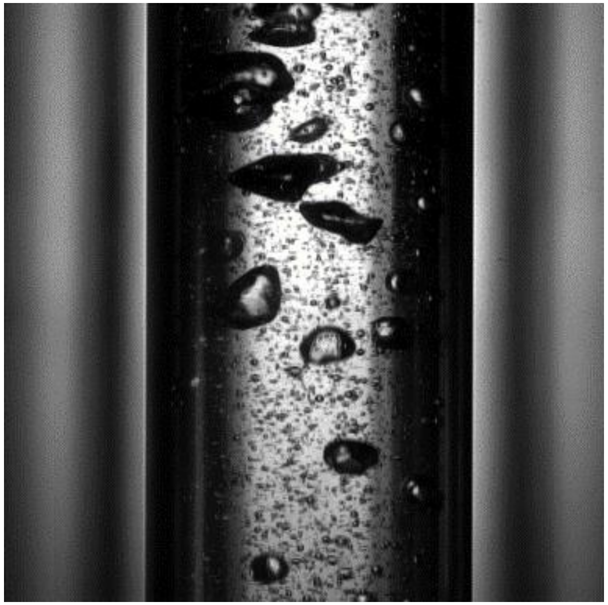

Two-phase flow image of CO_2 from David's vertical setup at CERN

How to approximate 3D bubbles statistically?

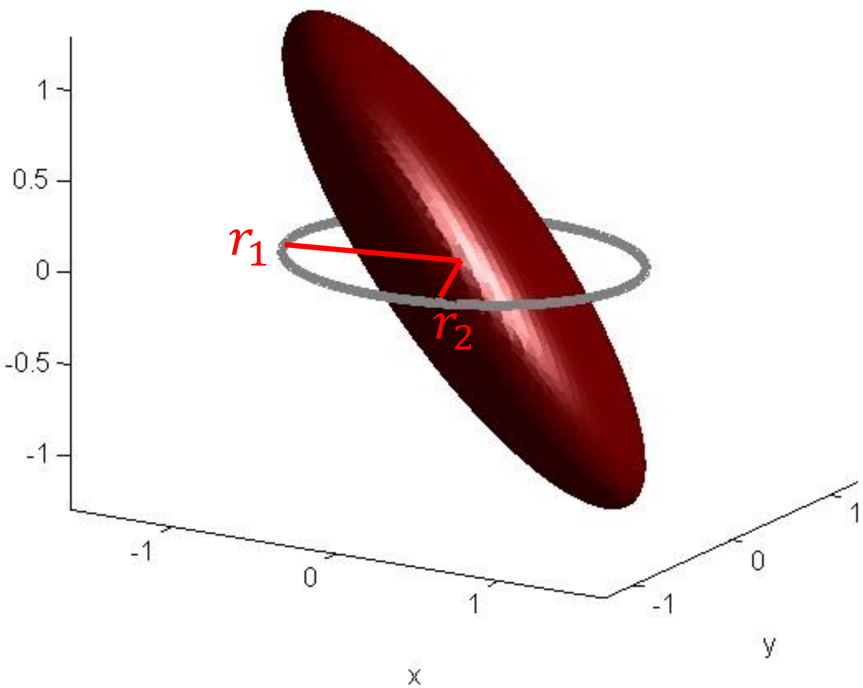

Ellipsoid semi-axis lengths: R_1, R_2, R_3
2D projection ellipse major &minor axes: r_1, r_2

$$R_1 \geq r_1 \geq r_2 \geq R_3$$

$$Volume = \frac{4}{3}\pi R_1 R_2 R_3 \approx VolumeApprox(r_1, r_2)$$

- Monte Carlo simulations can be used to create ellipsoids take projections and solve an inverse problem to approximate volume from the projected ellipses
- Similar Monte Carlo Simulations were used from estimating galaxy shapes (Binggeli 1980) to sand grain shapes (Yan et al. 2017)

Projection of an Ellipsoid

Ellipsoid equation: $\frac{x^2}{{R_1}^2} + \frac{y^2}{{R_2}^2} + \frac{z^2}{{R_3}^2} = 1 \Leftrightarrow \underline{\boldsymbol{X}}^{\boldsymbol{T}} \underline{\underline{\boldsymbol{A}}}\, \underline{\boldsymbol{X}} = 1$

where $\underline{X} \coloneqq \begin{bmatrix} x \\ y \\ z \end{bmatrix}$ *and* $\underline{\underline{A}} \coloneqq \begin{bmatrix} {R_1}^{-2} & 0 & 0 \\ 0 & {R_2}^{-2} & 0 \\ 0 & 0 & {R_3}^{-2} \end{bmatrix}$

Projection of an Ellipsoid

Ellipsoid equation: $\frac{x^2}{{R_1}^2} + \frac{y^2}{{R_2}^2} + \frac{z^2}{{R_3}^2} = 1 \Leftrightarrow \underline{\boldsymbol{X}}^{\boldsymbol{T}} \underline{\underline{\boldsymbol{A}}}\, \underline{\boldsymbol{X}} = 1$

$$\text{where} \quad \underline{X} \coloneqq \begin{bmatrix} x \\ y \\ z \end{bmatrix} \; and \; \underline{\underline{A}} \coloneqq \begin{bmatrix} {R_1}^{-2} & 0 & 0 \\ 0 & {R_2}^{-2} & 0 \\ 0 & 0 & {R_3}^{-2} \end{bmatrix}$$

Projection along unit projection vector $\underline{v} = \begin{bmatrix} n_x \\ n_y \\ n_z \end{bmatrix}$:

$$\underline{\boldsymbol{X}}^{\boldsymbol{T}} \underline{\underline{\boldsymbol{B}}}\, \underline{\boldsymbol{X}} = 1$$

$$\text{where } \underline{\underline{\boldsymbol{B}}} \coloneqq \underline{\underline{\boldsymbol{A}}} - \frac{\underline{\underline{\boldsymbol{A}}}\, \underline{\boldsymbol{v}}\, \underline{\boldsymbol{v}}^{\boldsymbol{T}} \underline{\underline{\boldsymbol{A}}}}{\underline{\boldsymbol{v}}^{\boldsymbol{T}} \underline{\underline{\boldsymbol{A}}}\, \underline{\boldsymbol{v}}}$$

$r_k = \frac{1}{\sqrt{\lambda_k}}$, k=1,2, and λ_k are eigenvalues of $\underline{\underline{\boldsymbol{B}}}$

Designing Monte Carlo Simulation

0.1 to 10 Million ellipsoids with a specific projection vector were generated by

- Choosing characteristic semi-axis length randomly between minimum detectable bubble radius 0.05 mm and inner radius of the tube 4 mm
- Choosing 5 as a maximum aspect ratio of the bubbles (observation from our images)
- Choosing semi-axis lengths randomly in an interval bounded by

```
infR =  max(characteristicR/sqrt(maximumAspectRatio=5),
                                    minimumDetectableBubbleRadius=0.5)

supR = min(characteristicR*sqrt(maximumAspectRatio=5),
                                               maximumBubbleRadius=4)
```

Creating Random Unit Projection Vector

$$n_x = \cos\theta \sin\varphi$$
$$n_y = \sin\theta \sin\varphi$$
$$n_z = \cos\varphi$$
$$where\ \theta \in [0, 2\pi), \varphi \in [0, \pi)$$

If θ *and* φ are uniformly distributed, the unit projection vector would not be random!

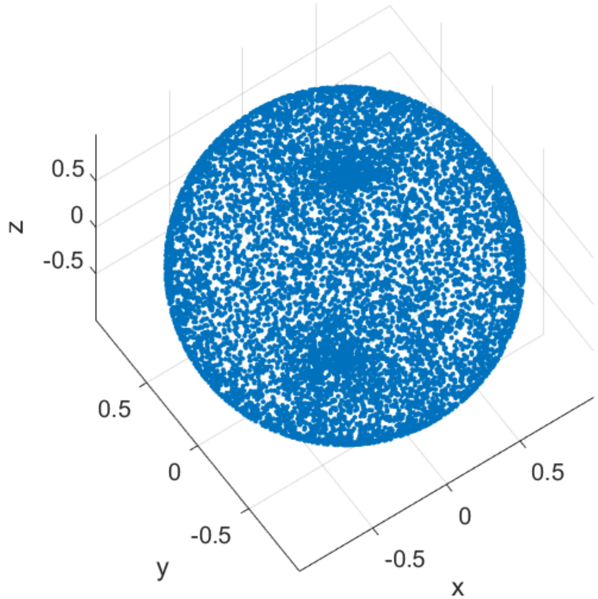

Creating Random Unit Projection Vector

$$n_x = \cos\theta \sin\varphi$$
$$n_y = \sin\theta \sin\varphi$$
$$n_z = \cos\varphi$$
$$where\ \theta \in [0, 2\pi), \varphi \in [0, \pi)$$

If θ and φ are uniformly distributed, the unit projection vector would not be random!

Creating random direction

$$\theta = 2\pi\zeta_1$$
$$\varphi = \arccos(1 - 2\zeta_2)$$

uniformly distributed random variables:

$\zeta_1\ \zeta_2 \in [0,1]$

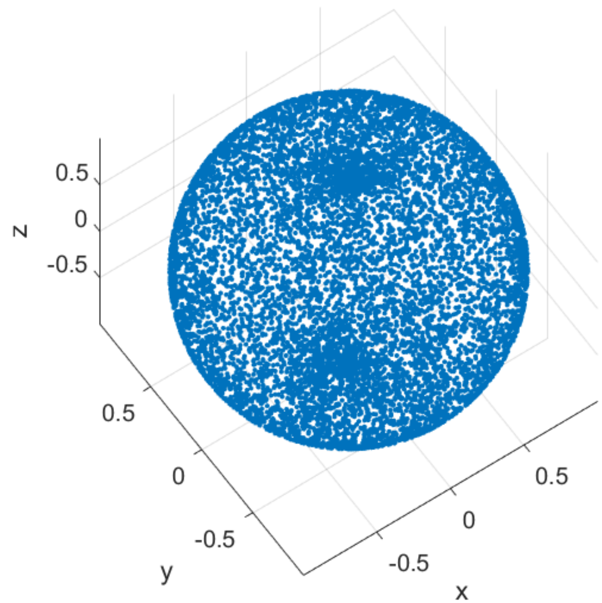

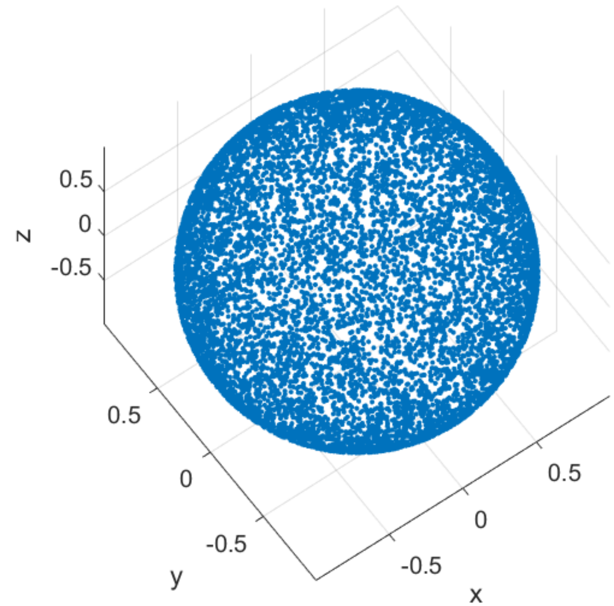

Arithmetic Mean Model with Monte Carlo

$$Mean\,Volume \approx MeanVolumeApprox\_Arithmetic(r_1, r_2)$$

$$\frac{1}{n}\sum_{i=1}^{n}\frac{4}{3}\pi {R_1}^i {R_2}^i {R_3}^i \approx C_{arithmetic}\frac{1}{n}\sum_{i=1}^{n}\frac{4}{3}\pi {r_1}^i {r_2}^i \frac{{r_1}^i + {r_2}^i}{2}$$

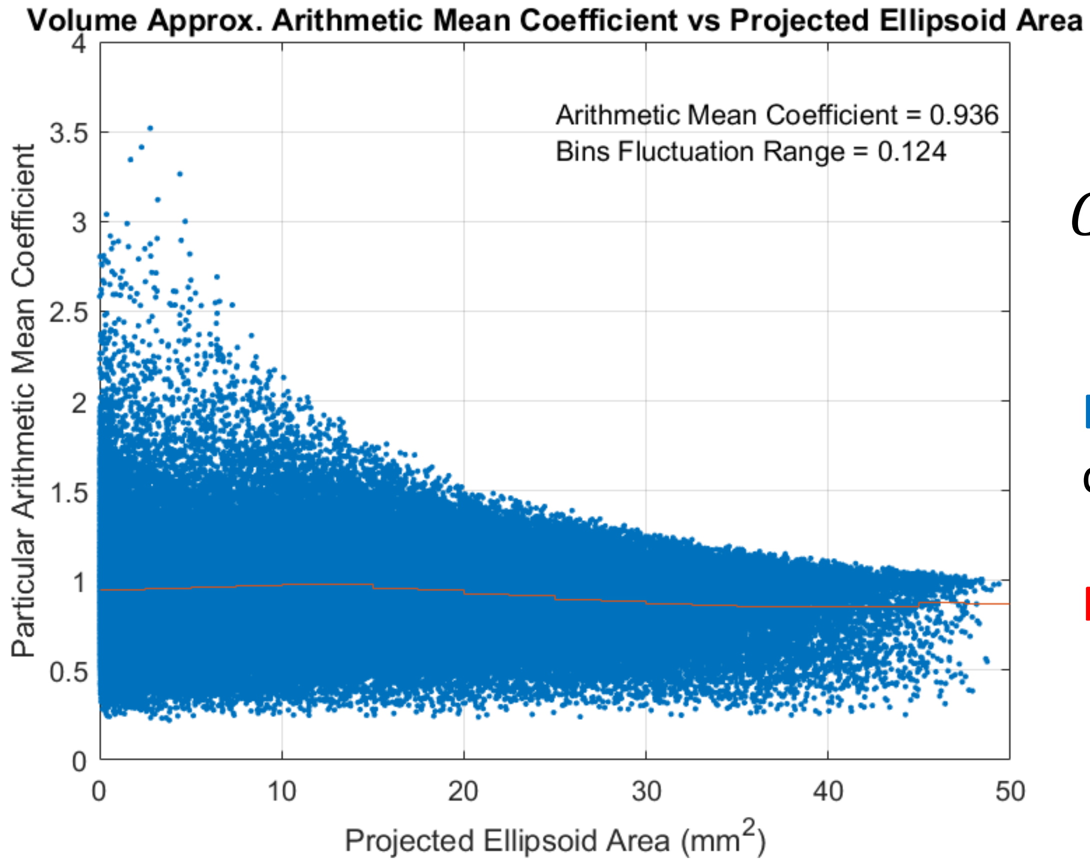

$$C_{arithmetic} \approx 0.936 \pm 6.6\%$$

Blue:
coefficient for a single ellipsoid

Red:
mean of the points in 20 bins

Geometric Mean Model with Monte Carlo

$$Mean\ Volume \approx MeanVolumeApprox\_Geometic(r_1, r_2)$$

$$\frac{1}{n}\sum_{i=1}^{n}\frac{4}{3}\pi {R_1}^i {R_2}^i {R_3}^i \approx C_{geometric}\frac{1}{n}\sum_{i=1}^{n}\frac{4}{3}\pi {r_1}^i {r_2}^i \frac{\sqrt{{r_1}^i {r_2}^i}}{2}$$

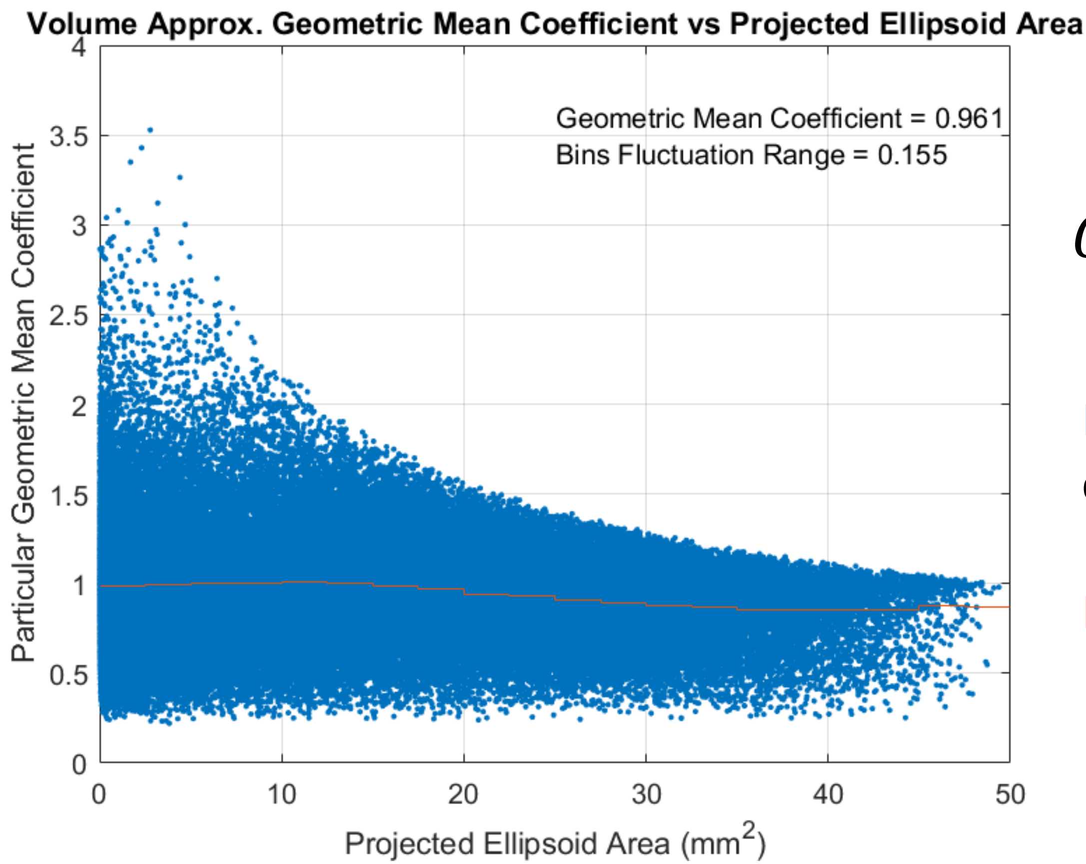

$$C_{geometric} \approx 0.961 \pm 8.1\%$$

Blue:
coefficient for a single ellipsoid

Red:
mean of the points in 20 bins

Harmonic Mean Model with Monte Carlo

$$Mean\,Volume \approx MeanVolumeApprox\_Harmonic(r_1, r_2)$$

$$\frac{1}{n}\sum_{i=1}^{n}\frac{4}{3}\pi {R_1}^i {R_2}^i {R_3}^i \approx C_{harmonic}\frac{1}{n}\sum_{i=1}^{n}\frac{4}{3}\pi {r_1}^i {r_2}^i \frac{2{r_1}^i {r_2}^i}{{r_1}^i + {r_2}^i}$$

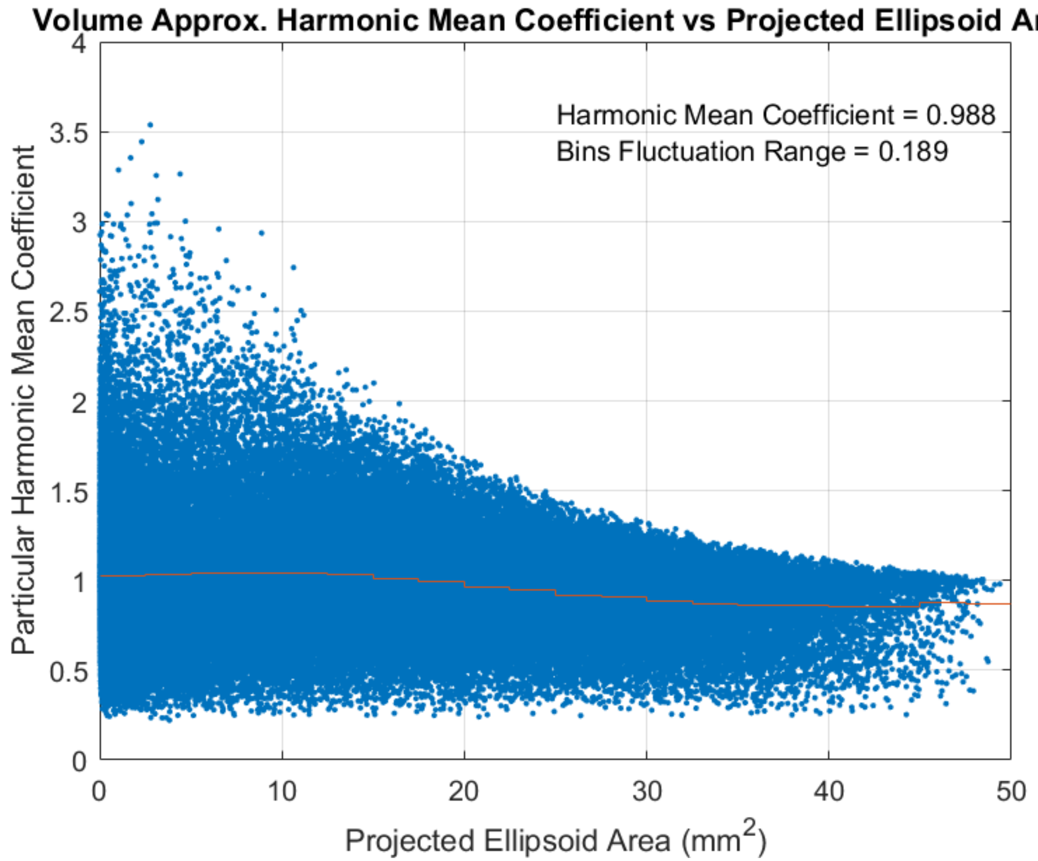

$$C_{harmonic} \approx 0.988 \pm 9.6\%$$

Blue:
coefficient for a single ellipsoid

Red:
mean of the points in 20 bins

L2 Mean Model with Monte Carlo

$$Mean\ Volume \approx MeanVolumeApprox\_L2(r_1, r_2)$$

$$\frac{1}{n}\sum_{i=1}^{n}\frac{4}{3}\pi {R_1}^i {R_2}^i {R_3}^i \approx C_{L2}\frac{1}{n}\sum_{i=1}^{n}\frac{4}{3}\pi {r_1}^i {r_2}^i \frac{\sqrt{({r_1}^i)^2+({r_2}^i)^2}}{\sqrt{2}}$$

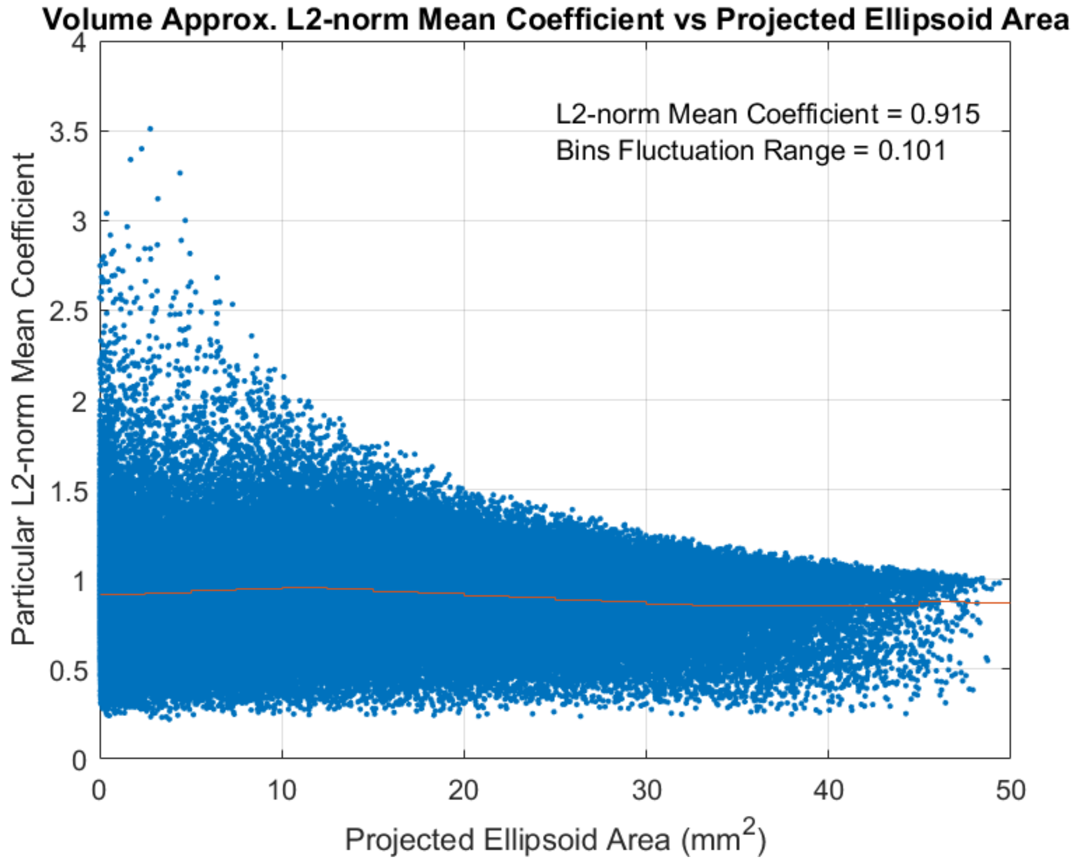

$$C_{L2} = 0.915 \pm 5.2\%$$

Blue:
coefficient for a single ellipsoid

Red:
mean of the points in 20 bins

Most Robust: L2 Mean Model

$$\mathit{Minimum\ Bins\ Fluctuation}\ (\text{L2 Mean Model with } \pm 5.2\%) \Leftrightarrow$$
$$\mathit{The\ most\ robust\ for\ changing\ bubble\ sizes}$$

$$Mean\,Volume \approx MeanVolumeApprox\_L2(r_1, r_2)$$

$$\frac{1}{n}\sum_{i=1}^{n}\frac{4}{3}\pi {R_1}^{i}{R_2}^{i}{R_3}^{i} \approx 0.9143\,\frac{1}{n}\sum_{i=1}^{n}\frac{4}{3}\pi {r_1}^{i}{r_2}^{i}\,\frac{\sqrt{({r_1}^{i})^2 + ({r_2}^{i})^2}}{\sqrt{2}}$$

Artificial Neural Networks (ANN)

- Training ANN with 2 inputs (r_1, r_2) to estimate 1 output (volume) would provide more sophisticated functions and more accurate results
- 10 Million data points, Training with Levenberg-Marquardt Algorithm 70% training, 15% testing, 15% validation

$$Volume \approx VolumeApprox(r_1, r_2)$$
$$with\ R = 0.9484\ (Regression\ R\ value > 0.93\ indicates\ strong\ correlation)$$

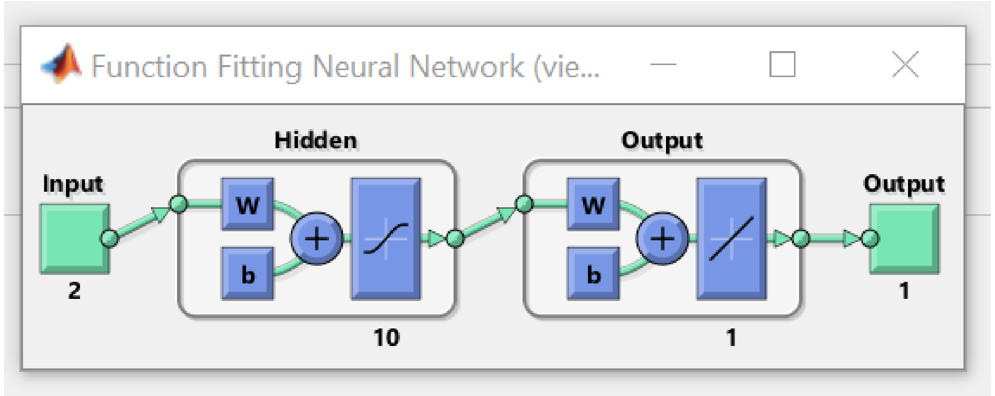

MATLAB nftool - Network Architecture

Artificial Neural Networks (ANN)

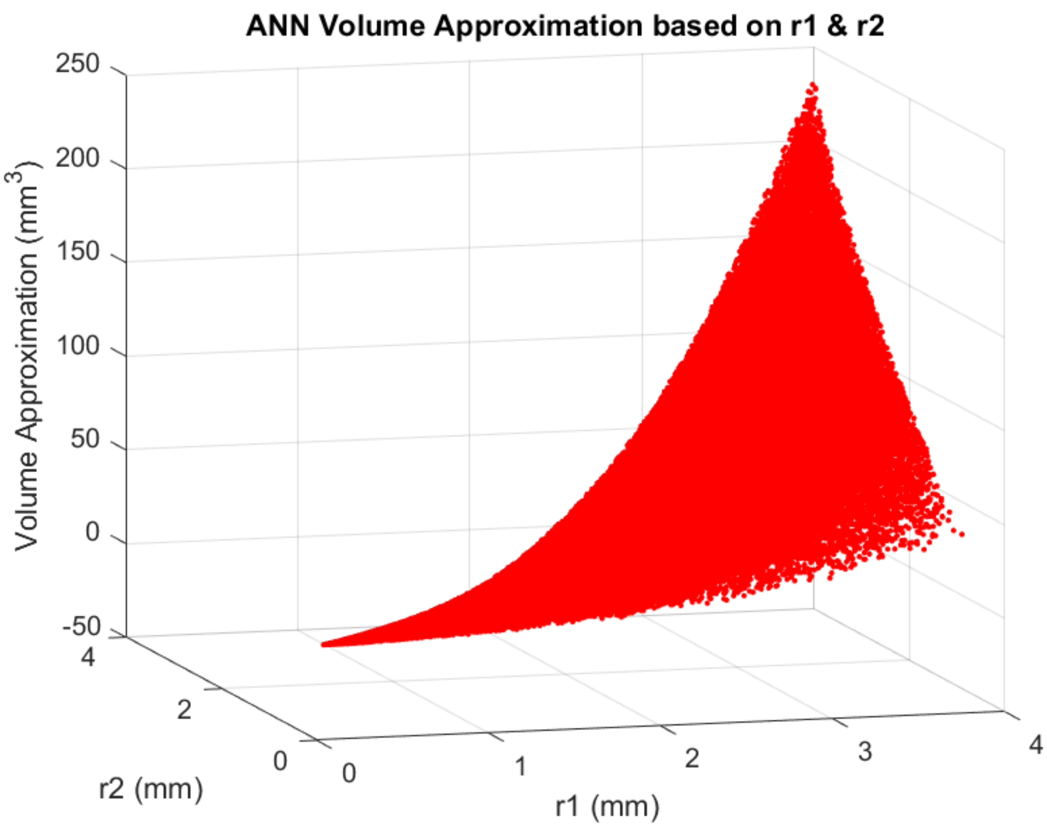

100 k data points

L2-norm Error: 0.1462%

ANN Error: $4.5 \cdot 10^{-4}\%$

ANN will perform significantly better then other models if there are only smaller bubbles or bigger bubbles

As a next step, big dataset of (r_1, r_2) of high-speed camera images can be used to make Monte Carlo simulation fully data driven

Outlook: Other Flow Regimes with Median Filter

- Median filter can be used on high-speed camera images to understand flow characteristic
- One can implement classification based on training CNN with median filtered images and Power Spectral Density (PSD)

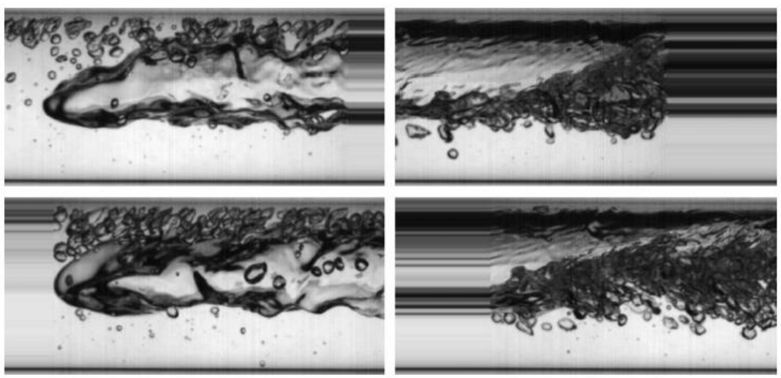

Fig. 7. Bubble noses and tails from top and bottom of Fig. 5 after synchronization and gap filling. The horizontal stripe-like pattern is caused by the replication.

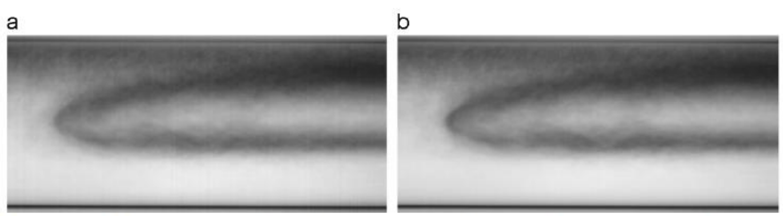

Fig. 8. Mean of 165 pictures of bubble noses after (a) ℓ_1 and (b) ℓ_2 synchronizations. We can note that ℓ_2 synchronization provides a slightly better visual quality, i.e. nose tip is less blurred.

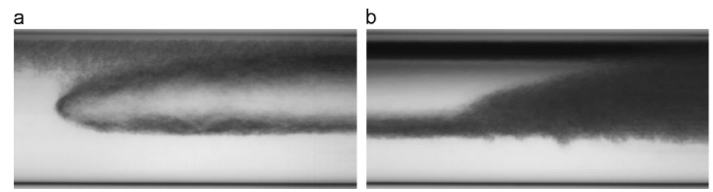

Fig. 9. Median of 165 pictures of bubble nose and tail after ℓ_2 synchronization.

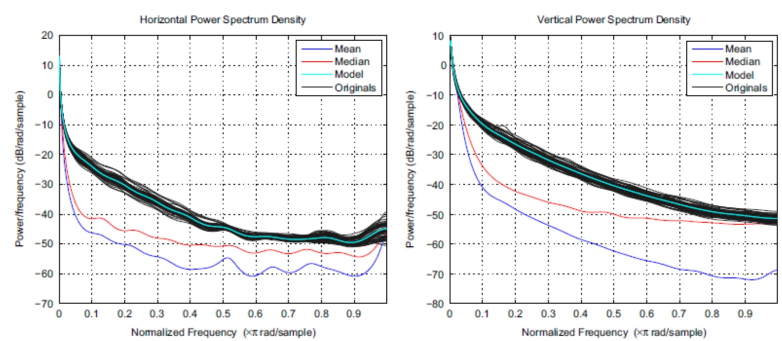

Fig. 10. PSD's of bubble noses. Individual bubble pictures (overlapped gray curves) have much richer frequency content than their mean and median counterparts. "Model" stands for mean PSD.

Ripa et Al. 2014, Typical bubble shape estimation in two-phase flow using inverse problem techniques

Outlook: Laser Attenuation Technique

$$I = I_0 \times e^{-\mu d}$$

$$I_{norm} = \frac{I - I_l}{I_g - I_l}$$

$$\alpha = \frac{1}{N}\sum_{n=1}^{N} I_{norm}$$

I, I_g, I_l: Intensities of the laser beams passing through two−phase flowor pure liquid or gas

α: Void Fraction Ratio

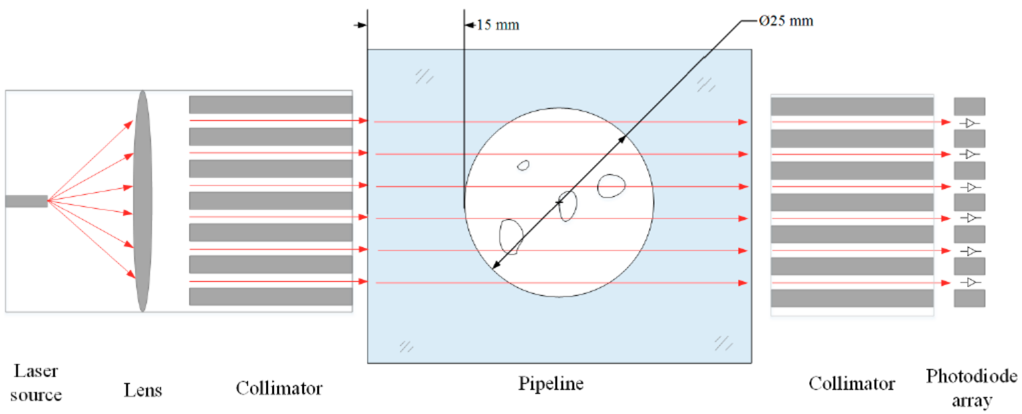

Figure 1. The structure of the sensing configuration.

Figure 5. Photo of the observation window.

Wu et al. 2019, Gas Void Fraction Measurement of Gas-Liquid Two-Phase CO2 Flow Using Laser Attenuation Technique

References

1. Taubin 1991 - Estimation of Planar Curves, Surfaces, and Nonplanar Space Curves Defined by Implicit Equations with Applications to Edge and Range Image Segmentation
2. Binggeli 1980 - On the Intrinsic Shape of Elliptical Galaxies
3. Yan et al. 2017 - Inferring 3D particle size and shape characteristics from projected 2D images Lessons learned from ellipsoids
4. Ripa et Al. 2014, Typical bubble shape estimation in two-phase flow using inverse problem techniques
5. Wu et al. 2019, Gas Void Fraction Measurement of Gas-Liquid Two-Phase CO2 Flow Using Laser Attenuation Technique

THANK YOU ALL!